doi:10.1093/brain/awx319 BRAIN 2018: 0; 1–14 | 1

BRAIN
A JOURNAL OF NEUROLOGY

Asymmetry of post-mortem neuropathology in behavioural-variant frontotemporal dementia

David J. Irwin,[1,2,3] Corey T. McMillan,[1,2] Sharon X. Xie,[4] Katya Rascovsky,[1,2] Vivianna M. Van Deerlin,[5,6] H. Branch Coslett,[2,7] Roy Hamilton,[2,7] Geoffrey Aguirre,[2,7] Edward B. Lee,[3,5,6,8] Virginia M. Y. Lee,[3,5,6] John Q. Trojanowski[3,5,6,*] and Murray Grossman[1,2,*]

*These authors contributed equally to this work.

Antemortem behavioural and anatomic abnormalities have largely been associated with right hemisphere disease in behavioural-variant frontotemporal dementia, but post-mortem neuropathological examination of bilateral hemispheres remains to be defined. Here we measured the severity of post-mortem pathology in both grey and white matter using a validated digital image analysis method in four cortical regions sampled from each hemisphere in 26 patients with behavioural-variant frontotemporal dementia, including those with frontotemporal degeneration (i.e. tau = 9, TDP-43 = 14, or FUS = 1 proteinopathy) or Alzheimer's pathology ($n = 2$). We calculated an asymmetry index based on the difference in measured pathology from each left-right sample pair. Analysis of the absolute value of the asymmetry index (i.e. degree of asymmetry independent of direction) revealed asymmetric pathology for both grey and white matter in all four regions sampled in frontototemporal degeneration patients with tau or TDP-43 pathology ($P \leqslant 0.01$). Direct interhemispheric comparisons of regional pathology measurements within-subjects in the combined tauopathy and TDP-43 proteinopathy group found higher pathology in the right orbitofrontal grey matter compared to the left ($P < 0.01$) and increased pathology in ventrolateral temporal lobe grey matter of the left hemisphere compared to the right ($P < 0.02$). Preliminary group-wise comparisons between tauopathy and TDP-43 proteinopathy groups found differences in patterns of interhemispheric burden of grey and white matter regional pathology, with greater relative white matter pathology in tauopathies. To test the association of pathology measurement with ante-mortem observations, we performed exploratory analyses in the subset of patients with imaging data ($n = 15$) and found a direct association for increasing pathologic burden with decreasing cortical thickness in frontotemporal regions on ante-mortem imaging in tauopathy ($P = 0.001$) and a trend for TDP-43 proteinopathy ($P = 0.06$). Exploratory clinicopathological correlations demonstrated an association of socially-inappropriate behaviours with asymmetric right orbitofrontal grey matter pathology, and reduced semantically-guided category naming fluency was associated asymmetric white matter pathology in the left ventrolateral temporal region. We conclude that pathologic disease burden is distributed asymmetrically in behavioural-variant frontotemporal dementia, although not universally in the right hemisphere, and this asymmetry contributes to the clinical heterogeneity of the disorder. The basis for this asymmetric profile is enigmatic but may reflect distinct species or strains of tau and TDP-43 pathologies with propensities to spread by distinct cell- and region-specific mechanisms. Patterns of region-specific pathology in the right hemisphere as well as the left hemisphere may play a role in antemortem clinical observations, and these observations may contribute to antemortem identification of molecular pathology in frontotemporal degeneration.

1 Penn Frontotemporal Degeneration Center, Perelman School of Medicine, University of Pennsylvania, Philadelphia, PA 19104, USA
2 Department of Neurology, Perelman School of Medicine, University of Pennsylvania, Philadelphia, PA 19104, USA
3 Center for Neurodegenerative Disease Research, Perelman School of Medicine, University of Pennsylvania, Philadelphia, PA 19104, USA

Received April 28, 2017. Revised August 18, 2017. Accepted October 14, 2017.

4 Department of Biostatistics, Epidemiology and Informatics, Perelman School of Medicine, University of Pennsylvania, Philadelphia, PA 19104, USA
5 Alzheimer's Disease Core Center, Perelman School of Medicine, University of Pennsylvania, Philadelphia, PA 19104, USA
6 Department of Pathology and Laboratory Medicine, Perelman School of Medicine, University of Pennsylvania, Philadelphia, PA 19104, USA
7 Center for Cognitive Neuroscience, Perelman School of Medicine, University of Pennsylvania, Philadelphia, PA 19104, USA
8 Translational Neuropathology Research Laboratory, Perelman School of Medicine, University of Pennsylvania, Philadelphia, PA 19104, USA

Correspondence to: David J. Irwin, MD
Frontotemporal Degeneration Center (FTDC)
University of Pennsylvania Perelman School of Medicine
Hospital of the University of Pennsylvania
3600 Spruce Street, Philadelphia, PA 19104
E-mail: dirwin@pennmedicine.upenn.edu

Correspondence may also be addressed to: Murray Grossman, MD
E-mail: mgrossma@pennmedicine.upenn.edu

John Q. Trojanowski, MD PhD
Center for Neurodegenerative Disease Research (CNDR)
University of Pennsylvania Perelman School of Medicine
Hospital of the University of Pennsylvania
3600 Spruce Street, Philadelphia, PA 19104
E-mail: trojanow@upenn.edu

Keywords: frontotemporal degeneration; tauopathy; TDP-43 proteinopathy; digital image analysis histology; behavioural variant frontotemporal dementia

Abbreviations: %AO = per cent area occupied; AI = asymmetry index; bvFTD = behavioural-variant frontotemporal dementia; FTLD = frontotemporal lobar degeneration; FTLD-Tau = FTLD with tau pathology; FTLD-TDP = FTLD with TDP-43 pathology; FTLD-FUS = FTLD with FUS pathology; INS = insula; OFC = orbitofrontal cortex; PPA = primary progressive aphasia; SPL = superior parietal lobule; VLT = ventral-lateral temporal lobe

Introduction

The behavioural-variant of frontotemporal dementia (bvFTD) (Rascovsky *et al.*, 2011) is a clinical syndrome characterized by a social comportment disorder often associated with cognitive difficulties, largely in executive functioning. BvFTD is the most common clinical phenotype caused by frontotemporal lobar degeneration (FTLD) neuropathology (Forman *et al.*, 2006) and is a common form of 'young-onset' dementia in patients under the age of 65 (Rossor *et al.*, 2010). Less commonly, atypical variants of Alzheimer's disease neuropathology, can also present with a bvFTD clinical syndrome (Forman *et al.*, 2006; Ossenkoppele *et al.*, 2015).

Neuroimaging studies in FTLD report varying degrees of asymmetry in cortical disease burden in patients with a specific molecular pathology (Whitwell *et al.*, 2005; Rohrer *et al.*, 2011), including those with underlying tauopathy (FTLD-Tau) or TDP-43 proteinopathy (FTLD-TDP) (Mackenzie *et al.*, 2010) and those constrained to clinical bvFTD suggest that the disease may have a propensity for affecting the right hemisphere, particularly ventral frontal regions (Seeley *et al.*, 2008; Whitwell *et al.*, 2009). Further, measures of social cognition in bvFTD, such as behavioural disinhibition (Mychack *et al.*, 2001; Liu *et al.*, 2004; Massimo *et al.*, 2009; Grossman *et al.*, 2010; Eslinger *et al.*, 2011; Powers *et al.*, 2014), loss of empathy and perspective-taking (Rankin *et al.*, 2006; Eslinger *et al.*, 2011; McMillan *et al.*, 2013*a*; Healey *et al.*, 2015), hyperorality (Woolley *et al.*, 2007) and apathy (Massimo *et al.*, 2009, 2015; Powers *et al.*, 2014) have neuroimaging correlates in frontotemporal regions largely in the right hemisphere. However, patients with bvFTD also frequently have clinical deficits in executive functioning such as category naming fluency, and these impairments appear to be less clearly lateralized, with findings associated with frontal and temporal regions in both right and left hemispheres, depending on the specific task (Rascovsky *et al.*, 2007; Libon *et al.*, 2009; Cook *et al.*, 2014).

Since there are no validated measures to define pathology in bvFTD during life, neuropathological examination and clinical-pathological correlation remain the gold standard to study the anatomic distribution and clinical consequences of abnormal protein aggregations within the nervous system that characterize the neuropathological substrate of this clinical syndrome. With rare exception, neuropathological examination typically assesses a single hemisphere, and moreover uses ordinal ratings of the

severity of pathology. These factors significantly limit the ability to validate reported asymmetries in antemortem disease burden in FTLD. Thus, there exists a substantial gap in the medical literature regarding the distribution of microscopic FTLD neuropathology within the CNS.

We hypothesize that the microscopic density of FTLD pathology associated with clinical bvFTD is not evenly distributed between cerebral hemispheres and these asymmetries may relate to antemortem clinical features. We also hypothesize that FTLD-Tau has higher white matter pathology compared to FTLD-TDP and this may influence hemispheric asymmetry of disease burden. Here, we provide novel examination of the inter hemispheric distribution of post-mortem grey matter and white matter pathology in a relatively large cohort of well-characterized bvFTD patients using a validated method of digital image analysis of histopathology in FTLD (Irwin *et al.*, 2016*b*). We find that regional pathological analysis of both grey and white matter is asymmetric in bvFTD, but the asymmetry of pathology does not always implicate the right hemisphere, with significant interindividual variation for some regions. Moreover, we find preliminary data that suggest differences in asymmetry in grey and white matter between FTLD-Tau and FTLD-TDP, and we associate these lateralized pathological findings with antemortem clinical and imaging measures associated with bvFTD.

Materials and methods

Patients

Patients followed longitudinally by experienced bvFTD neurologists (H.B.C., R.H., G.A., M.G.) were followed to autopsy at the Penn Center for Neurodegenerative Disease Research (CNDR). Eligible subjects had a clinical diagnosis of bvFTD and available tissue sampled fresh at autopsy from both hemispheres ($n = 26$) from a continuing series of >900 autopsies on diverse neurodegenerative disorders performed between 2005–2016. Patients were followed clinically as part of a longitudinal observational study (NIA-funded P01AG017586-16) at the Penn Frontotemporal Degeneration Center. All procedures were performed with informed consent in accordance with local Institutional Review Board guidelines.

Neuropathological examination

Fresh tissue was sampled at autopsy in standardized regions for diagnosis according to a neuroanatomical atlas and fixed overnight in 10% neutral buffered formalin as described (Toledo *et al.*, 2014). Tissue was processed as described (Irwin *et al.*, 2016*b*), embedded in paraffin blocks and cut into 6 µm sections for immunohistochemical staining for tau, amyloid-β, TDP-43 and α-synuclein with well-characterized antibodies (Toledo *et al.*, 2014). Neuropathological diagnosis was performed by expert neuropathologists (J.Q.T., E.B.L.) using formal criteria (Mackenzie *et al.*, 2010; Montine *et al.*, 2012). We had 25 bvFTD patients with available tissue from both hemispheres (FTLD-TDP = 14, FTLD-Tau = 9, Alzheimer's disease = 2; Table 1). One additional case with ubiquitin-positive, TDP-43-negative inclusions was additionally stained for fused-in-sarcoma (FUS) protein and found to have FUS proteinopathy (FTLD-FUS). FTLD-Tau group included the following subtypes: Pick's disease ($n = 4$), progressive supranuclear palsy ($n = 3$), corticobasal degeneration ($n = 1$) and an unclassifiable tauopathy with *MAPT* mutation (FTDP-17) (Table 1). We analysed the less common neuropathology groups separately (Alzheimer's disease = 2, FTLD-FUS = 1) and FTLD-FUS was analysed using traditional ordinal assessment only due to the inability to validate digital methods in a single case. Seven FTLD-TDP cases and four cases with Pick's disease tauopathy were previously reported in models of disease progression in bvFTD (Brettschneider *et al.*, 2014; Irwin *et al.*, 2016*a*) and an additional seven FTLD-TDP cases were assigned stages according to this model (Table 1).

Genetic analysis

DNA was isolated from peripheral blood or frozen brain using standard methods. The FTLD-TDP group was genotyped for pathogenic mutations in *GRN* using PCR as described (Yu *et al.*, 2010) or a custom targeted next-generation sequencing panel for neurodegenerative diseases (MiND-Seq) (Toledo *et al.*, 2013) and the *C9orf72* repeat expansion using a modified repeat-primed PCR (Suh *et al.*, 2015). The FTLD-Tau group was genotyped for pathogenic mutations in *MAPT* using PCR (Irwin *et al.*, 2013) or MiND-Seq. One FTLD-Tau patient had a p.P301L *MAPT* mutation, three FTLD-TDP patients had a pathogenic *GRN* mutation and four FTLD-TDP patients had a pathogenic *C9orf72* repeat-expansion mutation (Table 1).

Bilateral hemisphere sampling

Fresh tissue was sampled from each hemisphere at the time of autopsy in regions previously associated with bvFTD (Liu *et al.*, 2004; Woolley *et al.*, 2007; Seeley *et al.*, 2008) including the insula (INS), orbitofrontal (OFC), and ventral-lateral temporal (VLT) lobes, as well as a more posterior region in the superior parietal lobule (SPL) expected to have mild pathology to capture the full spectrum of interhemispheric disease burden in bvFTD. Missing data in a minority of cases was due to limited sampling at the time of autopsy (INS = 3, OFC = 3, SPL = 2, VLT = 7). An additional patient (Case 19) had insufficient insula grey matter on one section and was included only for white matter analysis for insula. Sections were stained with immunohistochemistry for the specific primary proteinopathy: phosphorylated TDP-43 for FTLD-TDP (rat monoclonal TAR5P-1D3, p409/410; Ascenion) (Neumann *et al.*, 2009), phosphorylated tau for FTLD-Tau or Alzheimer's disease (AT-8; ThermoScientific) (Mercken *et al.*, 1992) and FUS for FTLD-FUS (anti-FUS; ProteinTech). We also stained Alzheimer's disease tissue for amyloid-β pathology (Nab228; CNDR) (Lee *et al.*, 2003). To reduce 'run-to-run' variation in staining, the left/right hemispheric pair for each region was stained in the same immunohistochemical run.

Digital image analysis of histology

Digital images of histology slides at $\times 20$ magnification were obtained using a Lamina (Perkin Elmer) slide scanning system.

Table 1 Patient groups

Case No.	Subtype	PMI (h)	Brain weight (g)	Genetic mutation	Braak	CERAD	FTLD phase	Secondary pathology[b]	Sex	Handedness	Age at onset	Age at death	Disease duration
FTLD-TDP													
1	A	19	1250	-	1	A	3	AGD, HpSCl	M	R	55	74	19
2	A	6	967	*GRN*	0	0	4	-	M	A	67	78	11
3	A	16	906	*GRN*	0	0	3	-	F	R	61	66	5
4	A	19	1021	*C9orf72*	1	0	3	-	M	R	64	76	12
5	B	17.5	1019	*C9orf72*	2	0	4	-	F	R	61	70	9
6	A	19	1011	-	0	0	3	AGD	F	UNK	67	77	10
7	B	12	1357	*C9orf72*	0	0	3	-	F	R	57	61	4
8	B[a]	21	1385	*C9orf72*	1	0	4	-	M	R	50	54	4
9	A	14	757	*GRN*	2	A	3	-	F	R	59	63	4
10	B	18	1244	-	1	0	3	-	M	R	48	54	6
11	C	-	1401	-	1	A	2	-	M	L	68	73	5
12	UNCLAS	18	1425	-	0	0	4	-	F	R	58	61	3
13	UNCLAS	6	1405	-	1	0	3	-	M	R	62	65	3
14	A	10	1364	*C9orf72*	0	0	2	HpScl, LBD(T)	M	L	50	60	10
FTLD-Tau													
15	CBD	19.5	1149	-	0	0	NA	-	F	R	49	56	7
16	FTDP-17	6	970	*MAPT*	0	0	NA	-	F	R	56	65	9
17	PiD	11	960	-	0	0	4	-	M	R	48	57	9
18	PiD	22	941	-	0	0	3	-	M	R	58	71	13
19	PiD	14	1011	-	0	0	4	-	M	R	57	72	15
20	PSP	5	1297	-	1	0	NA	LBD(T)	M	R	69	79	10
21	PiD	18	1266	-	0	0	3	-	M	R	54	58	4
22	PSP	3	1237	-	1	A	NA	-	M	L	80	83	3
23	PSP	19	1349	-	0	A	NA	-	M	R	70	73	3
FTLD-FUS													
24	FTLD-FUS	18	1241	-	0	0	NA	-	M	R	48	51	3
AD													
25	AD	17.5	1441	-	3	3	NA	-	M	R	52	57	5
26	AD	12	1169	-	3	3	NA	-	M	R	52	62	10

[a]Concomitant motor neuron disease (ALS-FTD).
[b]Level of Alzheimer's disease co-pathology is designated in Braak and CERAD columns.
A = ambidextrous; A–C = FTLD-TDP subtypes according to Mackenzie *et al.* (2011) criteria; AD = Alzheimer's disease; AGD = argyrophilic grain disease (limbic stage); CBD = corticobasal degeneration; FTDP-17 = frontotemporal dementia with Parkinsonism and *MAPT* mutation; HPScl = hippocampal sclerosis; L = left-handed; LBD (T) = transitional stage Lewy body disease. FTLD phase refers to proposed staging system for FTLD-TDP (Brettschneider *et al.*, 2014) and Pick's disease (Irwin *et al.*, 2016*a*) in bvFTD; NA = no staging scheme available for pathological subtype; PiD = Pick's disease; PSP = progressive supranuclear palsy; R = right-handed; UNCLASS = FTLD-TDP pathology not conforming to FTLD subtype criteria; UNK = unknown handedness.

Digital image analysis was performed with Halo digital image software v1.90 (Indica Labs) with validated grey matter sampling and thresholding algorithms for FTLD-Tau and FTLD-TDP (Irwin *et al.*, 2016*b*). Briefly, a transect-belt sampling method is performed to manually segment representative cortex to reduce bias from under- or over-representation of FTLD pathology in tangentially-oriented tissue (Armstrong and Cairns, 2012). To further reduce sampling bias, we used a user-independent random sampling strategy using random tile placement feature of the program to include 175 µm region of interest tiles for 30% of the total area (Supplementary Fig. 1) (Irwin *et al.*, 2016*b*). Finally, intensity thresholding algorithms were applied to regions of interest to detect the total % pixel area occupied (%AO) for tau, TDP-43 or amyloid pathology and the final measurement for each slide was derived from the average of the randomly selected regions of interest. We used a similar approach to sample white matter regions of interest with manual segmentation of adjacent deep white matter tracts on each slide with a rectangular selection tool and then created user-independent random sampling with 175 µm region of interest tiles for 30% of the total area (Supplementary Fig. 1). Since Alzheimer's disease pathology is largely restricted to grey matter we did not analyse white matter for these cases. Validation of %AO pathology measurements were performed by comparing these data with traditional ordinal scores obtained blinded to quantitative measurements as described (Irwin *et al.*, 2016*b*) (Supplementary Fig. 2).

Clinical data

The clinical records were reviewed by an experienced clinician (D.J.I.), blinded to the pathology data, and the onset of core clinical features of bvFTD (behavioural disinhibition, apathy, loss of empathy, ritualistic behaviour and hyperorality) were extracted, as described (Irwin *et al.*, 2016*a*). Patients were

evaluated at baseline on average 3.3 years (±2.8) after the reported onset of disease with an average of 5.1 (±3.8) longitudinal visits at our FTD Centre. The average time from last visit to death was 2.1 years (±2.7). All cases met published criteria for bvFTD at presentation (Rascovsky *et al.*, 2011) except three cases, which had a prominent social disorder with additional clinical features (Supplementary Table 1). Case 6 with sporadic FTLD-TDP type-A had prominent apathy and dysexecutive syndrome with parkinsonism and was evaluated only late in the disease course and prior to modern criteria, thus there was insufficient social history to meet full bvFTD criteria; Case 14 with *C9orf72*-positive FTLD-TDP type-A had a prodromal period with atypical parkinsonism for several years prior to developing a prominent social disorder consistent with bvFTD; and Case 15 with post-mortem CBD tauopathy presented with mixed expressive language and comprehension difficulties at first visit with core bvFTD features emerging soon after and within the first 3 years that remained the most prominent feature throughout disease course. The remaining patients with pathogenic mutations (Table 1) all met clinical criteria for bvFTD (Supplementary Table 1) and Case 8 with *C9orf72* expansion had co-occurring motor neuron symptoms of amyotrophic lateral sclerosis.

Available neuropsychological test scores for baseline evaluation were obtained from the Penn integrated neurodegenerative disease database (INDD) (Xie *et al.*, 2011). These include Folstein Mini-Mental Status Examination (MMSE), letter-guided category naming fluency (i.e. number of 'F' words generated in 60 s), semantically-guided category naming fluency (i.e. number of animals generated in 60 s) and digit-span (i.e. longest number of digits repeated in forward and backward sequences). We obtained normative scores for these tests from an age- and education-matched cohort of healthy control patients in INDD ($n = 23$) to derive z-scores for patient performance.

Neuroimaging

Fifteen patients had antemortem T_1 structural MRI data available for analysis. Mean MRI–autopsy interval was 2.8 years (range 0–6 years) (Supplementary Table 5). All volumetric data were acquired on a Siemens 3.0 T Trio scanner at a resolution of $0.98 \times 0.98 \times 1$ mm. MRI data were processed using the ANTS cortical thickness pipeline as previously reported (Tustison *et al.*, 2014). We then computed mean cortical thickness in robust, neuroanatomically-defined regions of interest from a publicly-available atlas (Klein and Tourville, 2012) that map onto the anatomical regions sampled at autopsy, as described previously (Irwin *et al.*, 2016*a*). To determine the degree of cortical thinning in each region of interest we derived a z-score based on a demographically comparable ageing cohort (54 males, 97 females) without psychiatric or neurological history (age mean = 62.9 ± 7.3, mean education = 15.5 ± 2.9).

Statistical analysis

Direction-independent asymmetry index

Interhemispheric differences in pathologic burden were compared using a ratio (i.e. 'asymmetry index') of the difference in pathologic burden to the average burden between hemispheres in each region to account for absolute differences in %AO between FTLD subtypes:

Asymmetry index (AI) = (%AO pathology left hemisphere – %AO pathology right hemisphere) / (average %AO pathology left plus right hemispheres) × 100.

AI data were found to be normally distributed. To test for overall asymmetry of pathology across patients, independent of left/right directionality, we performed one-sample *t*-tests for the absolute value of AI for the null-hypothesis = 0. For a more conservative measure of asymmetry, we also compared the lower limit of the 95% confidence interval (CI) of each region of interest absolute value AI compared to the null hypothesis = 0.

Direction-dependent interhemispheric %AO measurement

Quantification of tau and TDP-43 pathology (%AO values) were not normally distributed. To test for group-level asymmetry of pathology to a particular hemisphere we performed a Wilcoxon matched-pair signed rank test comparing the left-right difference in %AO pathology per individual for each region.

Grey matter/white matter and clinicopathological correlations

A linear mixed-effects model procedure (Laird and Ware, 1982) was used to test the association of individual slide grey matter %AO as the dependent variable and white matter %AO as an independent variable to account for correlations among grey matter %AO in multiple regions sampled within the same patient. A random intercept term was included in the mixed-effects model. Fixed-effects independent variables included region and hemisphere sampled while controlling for fixed-effects co-variates for the presence of pathogenic mutation and disease duration. A similar model was used to test the association of regional MRI z-scores of CT on the dependent variable, pathology %AO measurement, including region and hemisphere as fixed effects independent variables and sex, presence of a pathogenic mutation, age and time to death (years) from MRI as fixed-effects covariates.

To quantify social disorder associated with bvFTD, we took the total number of three categories of behavioural disinhibition according to diagnostic criteria record (i.e. socially inappropriate behaviour, loss of manners/decorum and impulsivity; (Rascovsky *et al.*, 2011) reported in the record and categorized into severe ($\geqslant 2$ features present) or mild (< 2 features present). As detailed in the 'Results' section below, patients were characterized as right-predominant if grey matter pathology AI values were < 0.5 standard deviation (SD) of the absolute value of AI for grey matter (i.e. for OFC, grey matter AI $\leqslant -18.5$) and left-predominant if white matter pathology AI values were greater than 0.5 SD of the absolute value of AI for white matter (i.e. for VLT, white matter AI $\geqslant 20.4$) for clinicopathological correlations.

All other comparisons and correlations were performed using parametric and non-parametric analyses as appropriate. All analyses were performed using SPSS version 21.0 (IBM Corp., Armonk NY, USA) with two-tailed statistics ($P < 0.05$), except for individual region absolute value AI analyses, for which we used a more conservative $P \leqslant 0.01$ to control for multiple comparisons.

Results

Patients

Demographic data are presented in Table 1. The mean (±SD) post-mortem interval was 14.4 h (±5.6) and brain weight averaged 1174.7 g (±195.8). The mean age at onset = 58.5 years (±8.2), mean age at death = 66.0 years (±9.0) and disease duration = 7.5 years (±4.3). There was no significant difference between FTLD-TDP and FTLD-Tau groups in these variables ($P > 0.3$), which were similar to the FTLD-FUS and Alzheimer's disease cases.

Patients were impaired on all cognitive measures compared to a cohort of age- and education-matched healthy controls ($P < 0.001$) with a range in global cognitive performance at baseline (mean MMSE $z = -8.1 \pm 7.5$, range = 0, −20) and universal impairment in executive-mediated tasks (mean letter-guided verbal fluency $z = -1.6 \pm 0.7$, mean semantically-guided category fluency $z = -2.6 \pm 0.9$, mean digits backwards $z = -1.8 \pm 0.8$) and attention (mean digits forward $z = -2.3 \pm 1.1$) consistent with a clinical diagnosis of bvFTD (Supplementary Table 2).

Subsequent analyses focus on the majority of our patients who had either FTLD-Tau or FTLD-TDP pathology.

Overall hemispheric asymmetry of pathology in post-mortem tissue

Individual patient asymmetry may obscure measures of interhemispheric asymmetry in group-wise comparisons (e.g. equal numbers of right > left and left > right patients can create an average AI close to 0) (Rohrer *et al.*, 2011). Therefore, we first examined the absolute value of AI (i.e. a measure of asymmetry without left/right directionality) and found significant overall asymmetry in each individual sampled region (i.e. INS, OFC, SPL, VLT) ($P < 0.01$) (Fig. 1 and Table 2). Subset analyses of both sporadic (i.e. exclusion of patients with pathogenic mutation) and patients with pathogenic mutations alone found similar significant lateralization in both grey and white matter for each group in each region (all $P \leqslant 0.01$, data not shown).

Direction-specific regional hemispheric asymmetry in post-mortem tissue

Regional pathology measurement finds a higher median %AO of both tau and TDP-43 pathology burden for both right and left hemispheres in the frontotemporal regions sampled, with the area of lowest pathology in SPL (Fig. 2 and Supplementary Table 3). While we found little consistent evidence of direction-specific asymmetry between regions within an individual patient (see Supplementary Figs 3 and 4 that depict individual patient %AO and AI data for grey and white matter, respectively), we assessed group-level asymmetry of post-mortem pathology to a particular hemisphere in bvFTD for each region. In the total FTLD cohort, we found evidence for right greater than left hemisphere pathology in the OFC grey matter ($Z = 2.7$, $P < 0.01$) and left greater than right hemisphere pathology in VLT grey matter ($Z = 2.4$, $P = 0.02$) (Figs 2 and 3).

In preliminary pathological subgroup analyses, we found that the FTLD-Tau group has right greater than left OFC grey matter tau pathology ($Z = 2.5$, $P = 0.01$), and the FTLD-TDP group has right greater than left OFC white matter TDP-43 pathology ($Z = 2.4$, $P = 0.02$). There was a trend for increased left greater than right VLT grey matter pathology in the FTLD-TDP subgroup ($Z = 1.9$, $P = 0.06$) and FTLD-Tau subgroup ($Z = 1.8$, $P = 0.08$). There was no difference in right and left hemisphere pathology on group-

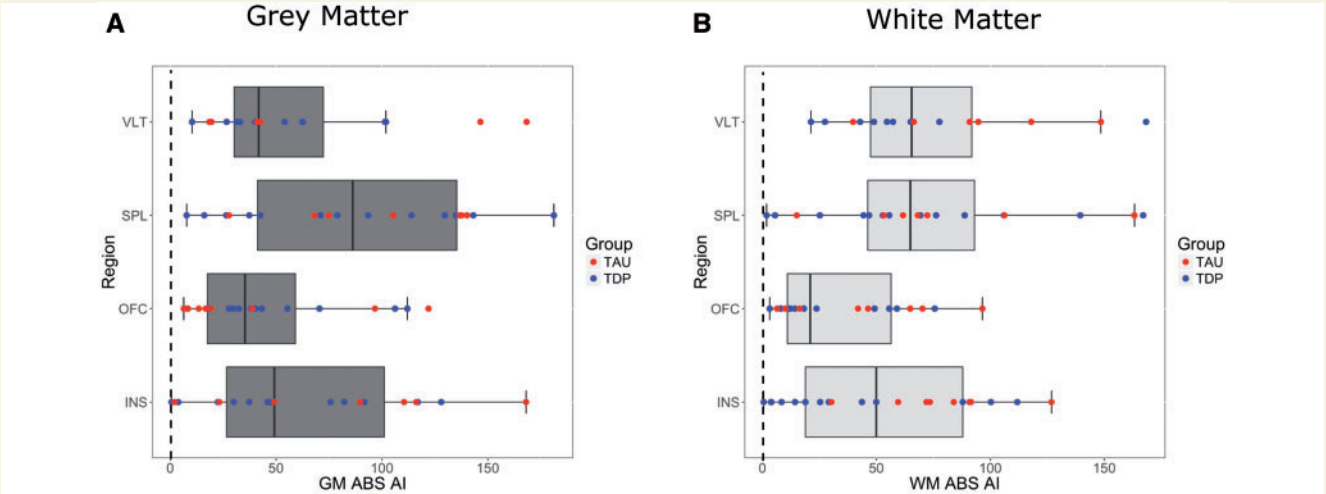

Figure 1 Direction-independent asymmetry of FTLD pathology in bvFTD. Boxplots with superimposed scatterplots of individual patient data coded by pathological diagnostic category depict the absolute value of the AI for each region sampled in (**A**) grey matter (GM) and (**B**) white matter (WM). Dashed lines represent the null hypothesis = 0 for symmetric pathology.

Table 2 Direction-independent group-wise assessment of hemispheric asymmetry of post-mortem FTLD pathology

Analysis	Region	Mean absolute value AI (95%CI)	Mean absolute value AI comparison to null = 0 T(df) *P*-value	Lower limit 95%CI mean absolute value AI comparison to null = 0 T(df) *P*-value
Grey matter pathology severity (%AO)	INS	65.3 (42.0–88.6)	5.9 (18) <0.001	3.8 (18) 0.001
	OFC	45.1 (27.9–62.4)	5.4 (19) <0.001	4.4 (19) <0.001
	SPL	88.3 (64.6–112.1)	7.8 (19) <0.001	5.7 (19) <0.001
	VLT	60.0 (35.3–84.7)	5.2 (15) <0.001	3.0 (15) 0.008
White matter pathology severity (%AO)	INS	53.6 (35.6–71.6)	6.2 (20) <0.001	4.1 (20) <0.001
	OFC	34.5 (21.3–47.7)	5.5 (19) <0.001	3.4 (20) 0.003
	SPL	70.9 (49.0–92.9)	6.8 (19) <0.001	4.7 (19) <0.001
	VLT	74.2 (52.2–96.3)	7.2 (15) <0.001	5.0 (15) <0.001

Table depicts results of one sample *t*-test comparing the mean and the lower limit of the absolute value of the asymmetry index (AI) for each region with the null-hypothesis mean = 0. Significant results suggest the distribution of pathology is not evenly distributed between left and right hemispheres.

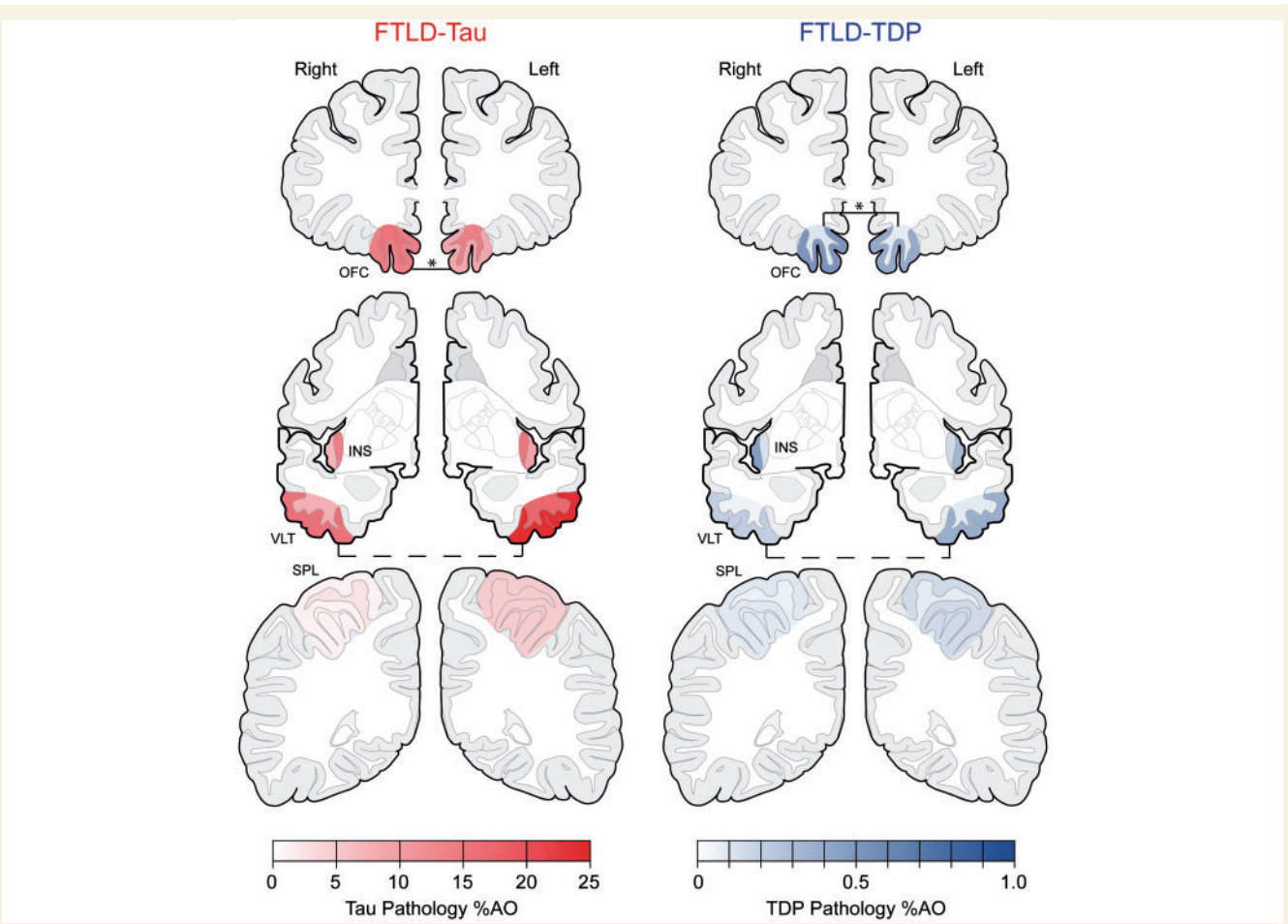

Figure 2 Heat map of regional pathological burden in bilateral hemispheres for bvFTD patients. Heat map depicts regional median %AO score for grey matter and white matter in four regions sampled for the FTLD-Tau (red) and FTLD-TDP (blue) subgroups. Scale bar depicts %AO colour shading intensity. Solid line with asterisk denotes $P < 0.05$ and dashed line with asterisk denotes $P = 0.06$–0.08 trend for paired Wilcoxon analysis of left/right hemisphere samples.

wise comparisons of SPL and INS (Supplementary Figs 3 and 4). Previous work has emphasized relatively greater white matter degeneration in FTLD-Tau than FTLD-TDP (McMillan *et al.*, 2013*b*), and we examined whether this is equally evident in regions of both hemispheres. First, we examined the association between grey matter and white matter pathology. Overall, we found increased individual slide grey matter %AO was associated with increased white matter %AO in both the FTLD-TDP ($\beta = 2.9$, SE = 0.3, df = 1, t = 9.8, $P < 0.001$) and somewhat less so for the

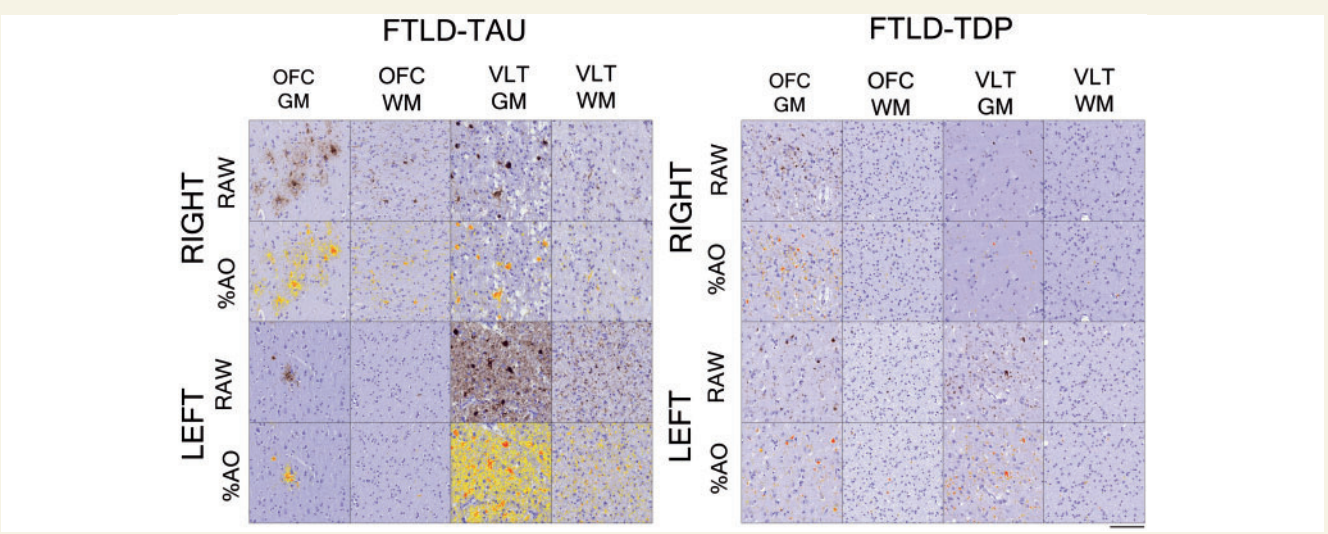

Figure 3 Photomicrographs of interhemispheric differences in the severity of FTLD neuropathology. Representative images depict raw images and %AO measurement (yellow/orange/red overlay) of lateralization of grey matter (GM) pathology in FTLD-Tau to the right orbitofrontal cortex in a progressive supranuclear palsy patient and left ventrolateral cortex in a patient with Pick's disease. FTLD-TDP type A case with more severe right orbitofrontal grey matter and white matter (WM) pathology than left hemisphere orbitofrontal cortex and more severe left ventrolateral temporal cortex grey matter and white matter compared to the right hemisphere homologous region. There is a higher proportion of total pathology in white matter in FTLD-Tau compared to FTLD-TDP. Scale bar = 100 μm.

FTLD-Tau subgroup ($\beta = 0.5$, SE = 0.1, df = 1, t = 4.4, $P < 0.001$). Next, we examined the %AO in paired grey matter-white matter samples from each slide and found in the FTLD-TDP group there was higher grey matter TDP-43 pathology %AO than in white matter for all regions in both hemispheres ($Z = 2.5$–3.1, all $P \leqslant 0.02$), while there was no significant difference in tau %AO in grey matter compared to white matter in any region for both hemispheres in FTLD-Tau ($Z < 1.6$, all $P > 0.05$).

Neuroimaging analysis

First, we examined the regional atrophy patterns in four regions of interest from antemortem MRI scans that approximate the same regions sampled at autopsy ($n = 15$). Similar to our pathology results, we found a high burden of atrophy in the frontotemporal regions (INS, OFC, VLT), with the more posterior SPL region having the least cortical atrophy (Supplementary Table 4). We next examined the relationship between antemortem cortical thinning and post-mortem %AO for tau and TDP-43 pathology for all available MRI-region of interest pairs in each hemisphere, and found a negative correlation of decreasing cortical thickness with increasing %AO of tau and TDP-43 pathology. This association appeared to be significant for FTLD-Tau ($\beta = -3.1$, SE = 0.8, df = 1, t = 3.7, $P = 0.001$), while we observed a trend in FTLD-TDP ($\beta = -0.1$, SE = 0.05, df = 1, t = 1.9, $P = 0.06$) (Fig. 4).

Clinicopathological correlation

To compare our pathology findings to cognitive/behavioural data, we tested the *a priori* hypothesis that more severe right OFC asymmetry would correspond to more severe behavioural disinhibition (Liu *et al.*, 2004; Viskontas *et al.*, 2007) and left VLT lateralization would be associated with worse performance on executive measures of category fluency (Libon *et al.*, 2009).

Patients with right-predominant pathology in OFC grey matter had a high degree of behavioural disinhibition (behaviour sum score $\geqslant 2$) (9/10 patients) compared to those with more symmetric or left-predominant OFC grey matter pathology (5/10 patients; $\lambda^2 = 3.8$, $P = 0.05$). These groups did not differ in the time interval from disease onset to first visit or from last visit to death ($t = 0.5$–1.4, $P > 0.1$). All but one patient with category fluency data available had left-predominant pathology in VLT grey matter so we examined VLT white matter for clinicopathological correlation. Comparison of patients with available neuropsychological test scores found those with left-predominant VLT white matter pathology ($n = 5$) had a lower score in semantically-guided category fluency (mean = 3.4 ± 1.9) compared to patients with more symmetric or right-predominant VLT white matter pathology ($n = 4$, mean = 10.5 ± 5.3; $P < 0.03$). Further, we found an inverse correlation with increasing VLT white matter AI values (increasing left-predominant pathology) with reduced semantically-guided category fluency scores ($n = 9$, $r = -0.66$, $P = 0.05$), but not letter-guided fluency scores ($n = 6$, $r = -0.03$, $P > 0.1$), indicating specificity for worse performance on category fluency related to the degree of asymmetry of VLT pathology to the left hemisphere. Further, FTLD-Tau and FTLD-TDP subgroups did not differ in category fluency scores (t = 0.6, $P > 0.5$) and VLT white matter asymmetry groups did not differ in

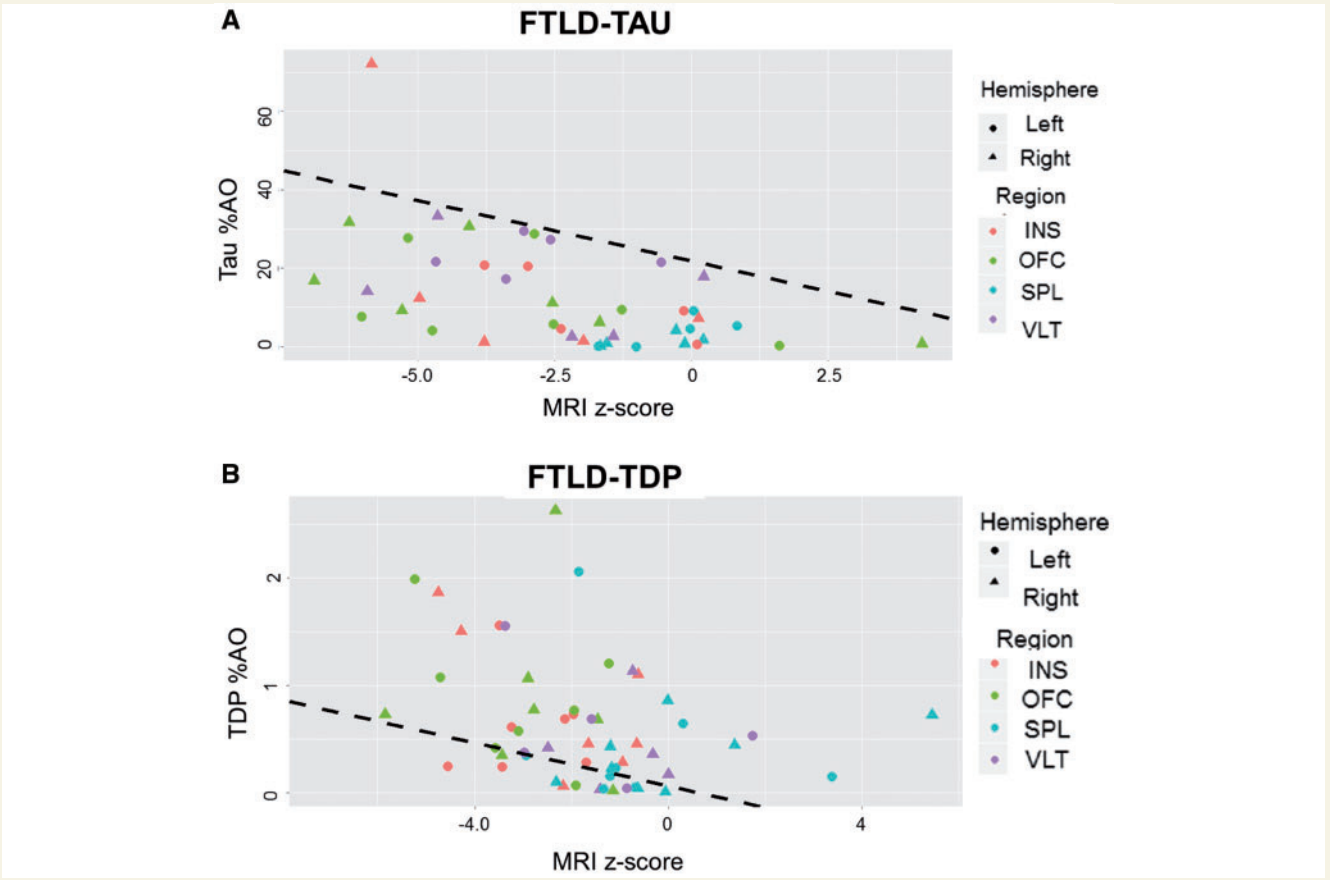

Figure 4 Association of antemortem neuroimaging data with post-mortem pathology measurement. Scatterplots depict individual data points for regional MRI CT z-scores plotted against post-mortem pathology %AO measurement in grey matter across hemispheres for (**A**) FTLD-Tau and (**B**) FTLD-TDP showing a direct association of antemortem MRI CT and post-mortem pathology severity. Dashed lines represent the estimated linear relationship between MRI and %AO from linear mixed-effects modelling including region and hemisphere as fixed-effects independent variables while controlling for fixed-effects covariates for sex, mutation status, age and duration from MRI to death. Colours code individual regions and shapes code for hemisphere sampled.

MMSE score, letter-guided fluency scores, age at testing or the interval from onset to testing (t = 0.1–1.3, $P > 0.05$).

Analysis of less common pathologies associated with bvFTD

Measurement of interhemispheric burden of pathology in our two patients with Alzheimer's disease found variable asymmetry that was largely congruent in directionality between tau and amyloid (Supplementary Table 4). SPL regions had similar or higher levels of tau and amyloid pathology compared to corresponding frontotemporal regions within each hemisphere. Qualitative examination of the single FTLD-FUS case found a higher severity of FUS-positive inclusion burden in the right (ordinal score = severe) > left (ordinal score = moderate) in OFC, while the VLT had severe FUS inclusion burden in the left hemisphere compared to moderate burden in the right hemisphere (Fig. 5). Finally, there was severe burden of pathology in the bilateral INS, while the SPL had lower burden of FUS pathology, which was at a moderate level in the right hemisphere compared to mild amounts in the left SPL.

Discussion

We report a novel digital neuropathological assessment of interhemispheric differences in pathology causing clinical bvFTD. We examined both grey and white matter pathological burden of tau and TDP-43 inclusions, and directly correlated pathological burden with antemortem imaging and clinical features. Pathology studies are critical because *in vivo* imaging methods to assess asymmetry in tauopathy (Chien *et al.*, 2013; Maruyama *et al.*, 2013) remain to be validated (Marquie *et al.*, 2015; Lowe *et al.*, 2016; McMillan *et al.*, 2016), and imaging ligands for FTLD-TDP or FUS are lacking. We discovered several novel findings. First, we found significant asymmetry of pathology overall in both grey and white matter. While bvFTD has been associated with more prominent right hemisphere disease, asymmetries in our pathology study implicated both right and left hemisphere regions in these patients. Regional

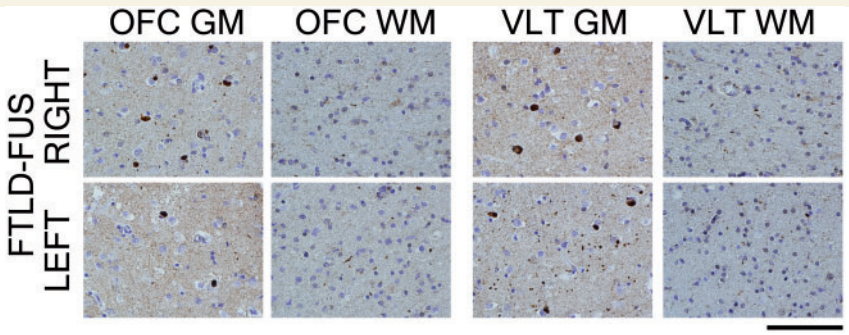

Figure 5 Photomicrographs of inter-hemispheric differences in the severity of FTLD-FUS patient. FTLD-FUS case shows some increase pathologic burden in the right orbitofrontal grey matter (GM) and left ventrolateral temporal cortex with rare white matter (WM) pathology overall. Scale bar = 100 μm.

comparisons thus revealed asymmetry of end-stage pathology to the right in OFC and left in VLT on group-level analysis, and increasing severity of post-mortem pathology measurement directly correlated with reduced antemortem cortical thickness on MRI. Moreover, we found converging evidence from exploratory clinicopathological observations in this bvFTD autopsy sample, where asymmetry in these regions was associated with antemortem clinical presentation in hemisphere-specific neuroanatomical substrates. Ratings of disinhibited behaviour were related to right-predominant OFC pathology, while performance on a measure of executive functioning that utilizes a temporal lobe-dependent semantic strategy was associated with left-predominant VLT pathology. These findings have important implications for future histopathological studies of FTLD.

The convention for neuropathological studies of neurodegenerative disease is microscopic examination of a single hemisphere. Very few studies have examined bilateral sampling in neurodegenerative disease and find minimal effects on diagnostic accuracy of Alzheimer's disease or dementia with Lewy bodies using qualitative ratings, but these studies included only rare FTLD patients (Stefanits *et al.*, 2012; King *et al.*, 2015). Quantitative assessments of interhemispheric burden of TDP-43 neuropathology in PPA patients with FTLD-TDP due to *GRN* mutations (Gliebus *et al.*, 2010; Kim *et al.*, 2016) found a predominance of pathology in language-related regions of the left hemisphere, but quantitative histopathological assessments have not been performed in bvFTD. In the present study, both FTLD-Tau and FTLD-TDP patients in our cohort had a higher burden of pathology in frontal and temporal regions than the more posterior parietal region sampled in both hemispheres (Supplementary Table 3 and Figs 2). While our observations are largely consistent with previous models of progressive histopathological burden in bvFTD performed within a single hemisphere (Brettschneider *et al.*, 2014; Irwin *et al.*, 2016*a*), the relative burden of pathology differed across hemispheres in frontal and temporal regions. Examination of regional pathological burden in a manner sensitive to interhemispheric sampling is not currently a component of FTLD neuropathological criteria (Mackenzie *et al.*, 2010). While more data are needed to make recommendations on the optimal regional sampling strategy across hemispheres for diagnostic purposes, and independent replication of our observation is required, we contend that regional asymmetry of pathology has important implications for FTLD research.

In the context of greater anterior disease burden in FTLD spectrum pathology, we found significant asymmetry of pathology in this cohort. Examination of the absolute value of AI revealed significant direction-independent asymmetry in all regions sampled, while direction-specific analyses found greater right than left grey matter pathology in OFC, and greater left than right grey matter pathology in VLT (Figs 2 and 3). These brain regions are thought to play a crucial role in the phenotypic expression of disease in FTD, as we discuss below. The basis for lateralization of pathology is unclear. The genetic and/or environmental aetiologies that influence the regional onset and progression of neurodegenerative disease are still speculative; however, premorbid neuroanatomic structure and intellectual skills or experiences also may influence the phenotypic expression of FTLD (Rogalski *et al.*, 2013; Placek *et al.*, 2016). It is possible that pathology accumulates in a lateralized manner as a unique property of these FTLD pathologies; however, left-lateralized neuropathology has been described in PPA patients with underlying Alzheimer's disease pathology as well (Mesulam *et al.*, 2014). In our two Alzheimer's disease patients with bvFTD we found variable asymmetry of pathology. Intra-hemispheric comparisons found SPL had similar or higher burden of pathology than frontotemporal regions sampled (Supplementary Table 4), which differed from our FTLD patients but is similar to previous neuroimaging findings in bvFTD with Alzheimer's disease pathology (Ossenkoppele *et al.*, 2015). Further study with larger groups of patients with both bvFTD and PPA due to Alzheimer's disease pathology are needed to fully compare interhemispheric patters of disease in Alzheimer's disease with FTLD.

While we found significant group-level asymmetry in this small cohort, it is important to keep in mind individual-patient variability in the regional pattern of asymmetry of post-

mortem pathology (Supplementary Figs 3 and 4). Beyond heterogeneity associated with different pathologies, there is also heterogeneity on directionality of asymmetry depending on the anatomic region that was sampled. Thus, there was group-level asymmetric pathology in OFC and VLT, but we did not find consistent lateralization of pathology to a particular hemisphere in both INS, which is thought to be an early site of structural degeneration in bvFTD (Seeley *et al.*, 2008), or SPL, which has minimal neurodegeneration on antemortem neuroimaging in most bvFTD patients (Seeley *et al.*, 2008; Rohrer *et al.*, 2011; Whitwell *et al.*, 2015). There may be regional differences in the hemisphere-specific progression of disease, and strains of pathological TDP-43 and tau may have different regional predilections also depending on the cell types affected, so these and other factors could influence the heterogeneity observed at end-stage disease. Likewise, neuroimaging studies of clinical bvFTD have reported several subgroups of patients with varying patterns of interhemispheric regional cortical atrophy (Whitwell *et al.*, 2009; Ranasinghe *et al.*, 2016), congruent with our pathological observations here. We did not find an association with overall hemispheric asymmetry and disease duration or pathology stage (data not shown); although we had only two patients who died with low (phase II) pathology (Table 1) and disease duration may not capture differences in rates of progression between individuals. Indeed, longitudinal neuroimaging data find differing rates of progression among molecular subtypes of FTLD across various regions (Rohrer *et al.*, 2011; Mahoney *et al.*, 2015; Whitwell *et al.*, 2015). Thus, our group-level analyses here may have limited generalizability to all forms of bvFTD.

We provide preliminary neuropathological data that show the proportion of overall pathology in white matter is higher for FTLD-Tau compared to FTLD-TDP in both hemispheres. Previously, in a cohort of autopsied FTLD patients with antemortem neuroimaging data, we found FTLD-Tau has a higher burden of white matter degeneration on MRI and in post-mortem evaluation compared to FTLD-TDP (McMillan *et al.*, 2013*b*) and studies of non-autopsied genetic forms of these diseases find more prominent white matter degeneration in *MAPT* patients compared to hereditary forms of FTLD-TDP (Mahoney *et al.*, 2014, 2015). While we accounted for influence of patients with pathogenic mutations, replication is needed in larger samples of each subtype of sporadic FTLD-Tau and FTLD-TDP to confirm these observations.

We emphasize that bvFTD is a clinically heterogeneous syndrome with diverse underlying neuropathological substrates. Previous studies found varying group-wise associations of clinical (Hu *et al.*, 2007; Mendez *et al.*, 2013) or neuroimaging features (Whitwell *et al.*, 2005) in rare autopsy-confirmed studies. Thus, there is no reliable way to differentiate these molecular pathologies during life (Irwin *et al.*, 2015). Here, we found preliminary evidence that distinct asymmetric patterns of tau and TDP-43 pathology across hemispheres may contribute to clinical heterogeneity on presentation, and thus detection of these features could potentially improve *in vivo* diagnostic accuracy of molecular pathology in bvFTD. Exploratory clinical-pathological correlations examined more closely the relationship between FTD phenotype during life and asymmetric FTLD pathology. Neurodegeneration in the right OFC has been associated with early symptoms of behavioural disinhibition (Liu *et al.*, 2004; Viskontas *et al.*, 2007; Seeley *et al.*, 2008; Grossman *et al.*, 2010) and may be one of the earliest sites for the deposition of TDP-43 pathology in bvFTD (Brettschneider *et al.*, 2014) and an early region of pathologic involvement in Pick's disease (Irwin *et al.*, 2016*a*). Our finding of increased social disinhibition during life in patients with more right-predominant pathology in OFC grey matter at autopsy suggests these patients may have had right-predominant OFC dysfunction during life, which remained evident microscopically at end-stage disease.

We also found a direct association of the degree of asymmetry with left-predominant VLT pathology with antemortem performance on a category-fluency task, which has neuroanatomical correlates in the temporal regions in the left hemisphere in bvFTD (Libon *et al.*, 2009; Cook *et al.*, 2014). This observation may reflect that some bvFTD patients have a phenotype that includes some features of semantic-variant PPA, especially those with a temporal-predominant presentation (Seeley *et al.*, 2005); however, only three of our patients developed single-word and object knowledge loss, as seen in semantic-variant PPA, and these patients had missing sampling for VLT so they were unfortunately not included in our analysis. Further, in our subset of patients with antemortem MRI, no patients had isolated VLT atrophy (Supplementary Table 5) suggestive of a temporal-variant of bvFTD (Whitwell *et al.*, 2009; Ranasinghe *et al.*, 2016). These findings begin to suggest the contribution of left hemisphere pathology to the clinical phenotype of bvFTD patients with temporal disease. Recent work has begun to emphasize the presence of subtle but statistically reliable langue deficits in non-aphasic patients with a bvFTD phenotype, and these deficits have been associated with both left hemisphere and right hemisphere changes in MRI regression analyses (Ash *et al.*, 2006; Charles *et al.*, 2014; Healey *et al.*, 2015; Cousins *et al.*, 2017). Future studies comparing the interhemispheric distributions of neuroanatomical variants of bvFTD, including patients with right-temporal predominant bvFTD and semantic-variant PPA (Gorno-Tempini *et al.*, 2011), which has predominant left temporal pathology, will be helpful to clarify the relationship between asymmetry of temporal lobe pathology at end-stage disease to antemortem origins of pathology.

Previous neuroimaging studies of autopsy-confirmed FTLD have not directly examined the relationship between severity of post-mortem pathology and antemortem grey matter atrophy (Whitwell *et al.*, 2005; Rohrer *et al.*, 2011), and quantitative study of FTLD-TDP in PPA has not examined antemortem MRI data (Kim *et al.*, 2016). Here, we found a novel direct association of antemortem quantitative MRI and post-mortem quantification of pathology. An important caveat is that MRI data were obtained

in our sample at a wide range of time intervals before the time of autopsy (<1 year to 6 years), and although we included time from MRI to death as a covariate in our model, we cannot exclude the possibility that differences in time of scanning and rate of progression of individual patients could contribute to the strength of association between antemortem imaging and post-mortem pathology.

The detection of these clinical-pathological correlations, as well as discovery of region-specific patterns of asymmetric pathological burden, was significantly facilitated by the digital pathological analysis used in this study (Irwin *et al.*, 2016*b*). Fine-grained ascertainment of pathological burden as a continuous variable, rather than a traditional ordinal scale, allowed subtler characteristics of histopathological observations to emerge as significant factors. Further, density of protein inclusions can be variable along the cortical ribbon and variation across adjacent tissue sections could influence assessments of asymmetry (King *et al.*, 2015). As such, we performed a user-independent, transect-belt sampling method (Supplementary Fig. 1) to reduce bias from variability in pathology density (Armstrong, 2003), which is not possible using subjective visual rating scales.

Several additional caveats should be considered in the interpretation of these results. First, despite our focus on clinical bvFTD to constrain neuroanatomical associations for group comparisons, our FTLD cohort was pathologically and genetically heterogeneous (Table 1), and molecular aetiologies of FTLD may have differing patterns of regional pathology and progression across hemispheres (Whitwell *et al.*, 2005; Rohrer *et al.*, 2011). Our bilateral sampling data are novel and represent over a decade of consecutive autopsy recruitment; however, due to the relative rarity of this disorder compared to more common neurodegenerative disease, the sample size does not permit analysis of individual subtypes of FTLD (i.e. A, B, C) (Mackenzie *et al.*, 2011) or FTLD-Tau (i.e. 4-repeat, 3-repeat) (Mackenzie *et al.*, 2010). Thus, we cannot generalize our specific regional findings of lateralization of right OFC and left VLT to all forms of bvFTD but instead we provide evidence of unequal inter-hemispheric distributions of microscopic pathology at end-stage disease. Although we sampled critical regions related to core clinical elements in bvFTD, we studied only a small number of regions and additional work is needed to study a larger sampling. Our clinical data were retrospective in nature, as such we had missing data for some neuropsychological measures and we cannot exclude the possibility that an unreported symptom in the record may have been present during the disease course.

With these caveats in mind, FTLD neuropathology associated with clinical bvFTD is asymmetric, although not always biased to the right hemisphere, and appears to have some regional specificity. These characteristics appear to contribute to the clinical heterogeneity of bvFTD. Further understanding of the divergent patterns of disease in molecular subtypes of FTLD are critical for the development of diagnostic biomarkers for aetiology-specific therapies in bvFTD.

Acknowledgements

We thank Manuela Neumann and Elisabeth Kremmer for providing the phosphorylation specific TDP-43 antibody p409/410. We thank Mary Leonard, Matthew Byrne, Felicia Cooper and Mendy Liang for their technical assistance. We thank Dr Gabor Kovacs for his thoughtful feedback on the manuscript. We would also like to thank the patients and their families, for without their meaningful contributions to medical research this work would not be possible.

Funding

This study was supported by NIH grants NS044266, AG038490, AG015116, AG010124, P01NS053488, P01AG032953, P01AG017586, AG043503, NS088341, Penn Institute on Aging and the Wyncote Foundation.

Supplementary material

Supplementary material is available at *Brain* online.

References

Armstrong RA. Quantifying the pathology of neurodegenerative disorders: quantitative measurements, sampling strategies and data analysis. Histopathology 2003; 42: 521–9.

Armstrong RA, Cairns NJ. Different molecular pathologies result in similar spatial patterns of cellular inclusions in neurodegenerative disease: a comparative study of eight disorders. J Neural Transm 2012; 119: 1551–60.

Ash S, Moore P, Antani S, McCawley G, Work M, Grossman M. Trying to tell a tale: discourse impairments in progressive aphasia and frontotemporal dementia. Neurology 2006; 66: 1405–13.

Brettschneider J, Del Tredici K, Irwin DJ, Grossman M, Robinson JL, Toledo JB, et al. Sequential distribution of pTDP-43 pathology in behavioral variant frontotemporal dementia (bvFTD). Acta Neuropathol 2014; 127: 423–39.

Charles D, Olm C, Powers J, Ash S, Irwin DJ, McMillan CT, et al. Grammatical comprehension deficits in non-fluent/agrammatic primary progressive aphasia. J Neurol Neurosurg Psychiatry 2014; 85: 249–56.

Chien DT, Bahri S, Szardenings AK, Walsh JC, Mu F, Su MY, et al. Early clinical PET imaging results with the novel PHF-tau radioligand [F-18]-T807. J Alzheimers Dis 2013; 34: 457–68.

Cook PA, McMillan CT, Avants BB, Peelle JE, Gee JC, Grossman M. Relating brain anatomy and cognitive ability using a multivariate multimodal framework. Neuroimage 2014; 99: 477–86.

Cousins KA, Ash S, Irwin DJ, Grossman M. Dissociable substrates underlie the production of abstract and concrete nouns. Brain Lang 2017; 165: 45–54.

Eslinger PJ, Moore P, Anderson C, Grossman M. Social cognition, executive functioning, and neuroimaging correlates of empathic deficits in frontotemporal dementia. J Neuropsychiatry Clin Neurosci 2011; 23: 74–82.

Forman MS, Farmer J, Johnson JK, Clark CM, Arnold SE, Coslett HB, et al. Frontotemporal dementia: clinicopathological correlations. Ann Neurol 2006; 59: 952–62.

Gliebus G, Bigio EH, Gasho K, Mishra M, Caplan D, Mesulam MM, et al. Asymmetric TDP-43 distribution in primary progressive aphasia with progranulin mutation. Neurology 2010; 74: 1607–10.

Gorno-Tempini ML, Hillis AE, Weintraub S, Kertesz A, Mendez M, Cappa SF, et al. Classification of primary progressive aphasia and its variants. Neurology 2011; 76: 1006–14.

Grossman M, Eslinger PJ, Troiani V, Anderson C, Avants B, Gee JC, et al. The role of ventral medial prefrontal cortex in social decisions: converging evidence from fMRI and frontotemporal lobar degeneration. Neuropsychologia 2010; 48: 3505–12.

Healey ML, McMillan CT, Golob S, Spotorno N, Rascovsky K, Irwin DJ, et al. Getting on the same page: the neural basis for social coordination deficits in behavioral variant frontotemporal degeneration. Neuropsychologia 2015; 69: 56–66.

Hu WT, Mandrekar JN, Parisi JE, Knopman DS, Boeve BF, Petersen RC, et al. Clinical features of pathologic subtypes of behavioral–variant frontotemporal dementia. Arch Neurol 2007; 64: 1611–16.

Irwin DJ, Brettschneider J, McMillan CT, Cooper F, Olm C, Arnold SE, et al. Deep clinical and neuropathological phenotyping of Pick disease. Ann Neurol 2016a; 79: 272–87.

Irwin DJ, Byrne MD, McMillan CT, Cooper F, Arnold SE, Lee EB, et al. Semi-automated digital image analysis of Pick's disease and TDP-43 proteinopathy. J Histochem Cytochem 2016b; 64: 54–66.

Irwin DJ, Cairns NJ, Grossman M, McMillan CT, Lee EB, Van Deerlin VM, et al. Frontotemporal lobar degeneration: defining phenotypic diversity through personalized medicine. Acta Neuropathol 2015; 129: 469–91.

Irwin DJ, Cohen TJ, Grossman M, Arnold SE, McCarty-Wood E, Van Deerlin VM, et al. Acetylated tau neuropathology in sporadic and hereditary tauopathies. Am J Pathol 2013; 183: 344–51.

Kim G, Ahmadian SS, Peterson M, Parton Z, Memon R, Weintraub S, et al. Asymmetric pathology in primary progressive aphasia with progranulin mutations and TDP inclusions. Neurology 2016; 86: 627–36.

King A, Bodi I, Nolan M, Troakes C, Al-Sarraj S. Assessment of the degree of asymmetry of pathological features in neurodegenerative diseases. What is the significance for brain banks? J Neural Transm 2015; 122: 1499–508.

Klein A, Tourville J. 101 labeled brain images and a consistent human cortical labeling protocol. Front Neurosci 2012; 6: 171.

Laird NM, Ware JH. Random-effects models for longitudinal data. Biometrics 1982; 38: 963–74.

Lee EB, Skovronsky DM, Abtahian F, Doms RW, Lee VM. Secretion and intracellular generation of truncated Abeta in beta-site amyloid-beta precursor protein-cleaving enzyme expressing human neurons. J Biol Chem 2003; 278: 4458–66.

Libon DJ, McMillan C, Gunawardena D, Powers C, Massimo L, Khan A, et al. Neurocognitive contributions to verbal fluency deficits in frontotemporal lobar degeneration. Neurology 2009; 73: 535–42.

Liu W, Miller BL, Kramer JH, Rankin K, Wyss-Coray C, Gearhart R, et al. Behavioral disorders in the frontal and temporal variants of frontotemporal dementia. Neurology 2004; 62: 742–8.

Lowe VJ, Curran G, Fang P, Liesinger AM, Josephs KA, Parisi JE, et al. An autoradiographic evaluation of AV-1451 Tau PET in dementia. Acta Neuropathol Commun 2016; 4: 58.

Mackenzie IR, Neumann M, Baborie A, Sampathu DM, Du Plessis D, Jaros E, et al. A harmonized classification system for FTLD-TDP pathology. Acta Neuropathol 2011; 122: 111–13.

Mackenzie IR, Neumann M, Bigio EH, Cairns NJ, Alafuzoff I, Kril J, et al. Nomenclature and nosology for neuropathologic subtypes of frontotemporal lobar degeneration: an update. Acta Neuropathol 2010; 119: 1–4.

Mahoney CJ, Ridgway GR, Malone IB, Downey LE, Beck J, Kinnunen KM, et al. Profiles of white matter tract pathology in frontotemporal dementia. Hum Brain Mapp 2014; 35: 4163–79.

Mahoney CJ, Simpson IJ, Nicholas JM, Fletcher PD, Downey LE, Golden HL, et al. Longitudinal diffusion tensor imaging in frontotemporal dementia. Ann Neurol 2015; 77: 33–46.

Marquie M, Normandin MD, Vanderburg CR, Costantino IM, Bien EA, Rycyna LG, et al. Validating novel tau positron emission tomography tracer [F-18]-AV-1451 (T807) on postmortem brain tissue. Ann Neurol 2015; 78: 787–800.

Maruyama M, Shimada H, Suhara T, Shinotoh H, Ji B, Maeda J, et al. Imaging of tau pathology in a tauopathy mouse model and in Alzheimer patients compared to normal controls. Neuron 2013; 79: 1094–108.

Massimo L, Powers C, Moore P, Vesely L, Avants B, Gee J, et al. Neuroanatomy of apathy and disinhibition in frontotemporal lobar degeneration. Dement Geriatr Cogn Disord 2009; 27: 96–104.

Massimo L, Powers JP, Evans LK, McMillan CT, Rascovsky K, Eslinger P, et al. Apathy in frontotemporal degeneration: neuroanatomical evidence of impaired goal-directed behavior. Front Hum Neurosci 2015; 9: 611.

McMillan CT, Coleman D, Clark R, Liang TW, Gross RG, Grossman M. Converging evidence for the processing costs associated with ambiguous quantifier comprehension. Front Psychol 2013a; 4: 153.

McMillan CT, Irwin DJ, Avants BB, Powers J, Cook PA, Toledo JB, et al. White matter imaging helps dissociate tau from TDP-43 in frontotemporal lobar degeneration. J Neurol Neurosurg Psychiatry 2013b; 84: 949–55.

McMillan CT, Irwin DJ, Nasrallah I, Phillips JS, Spindler M, Rascovsky K, et al. Multimodal evaluation demonstrates *in vivo* 18F-AV-1451 uptake in autopsy-confirmed corticobasal degeneration. Acta Neuropathol 2016; 132: 935–7.

Mendez MF, Joshi A, Tassniyom K, Teng E, Shapira JS. Clinicopathologic differences among patients with behavioral variant frontotemporal dementia. Neurology 2013; 80: 561–8.

Mercken M, Vandermeeren M, Lubke U, Six J, Boons J, van de Voorde A, et al. Monoclonal antibodies with selective specificity for Alzheimer Tau are directed against phosphatase-sensitive epitopes. Acta Neuropathol 1992; 84: 265–72.

Mesulam MM, Weintraub S, Rogalski EJ, Wieneke C, Geula C, Bigio EH. Asymmetry and heterogeneity of Alzheimer's and frontotemporal pathology in primary progressive aphasia. Brain 2014; 137 (Pt 4): 1176–92.

Montine TJ, Phelps CH, Beach TG, Bigio EH, Cairns NJ, Dickson DW, et al. National Institute on Aging-Alzheimer's Association guidelines for the neuropathologic assessment of Alzheimer's disease: a practical approach. Acta Neuropathol 2012; 123: 1–11.

Mychack P, Kramer JH, Boone KB, Miller BL. The influence of right frontotemporal dysfunction on social behavior in frontotemporal dementia. Neurology 2001; 56 (11 Suppl 4): S11–15.

Neumann M, Kwong LK, Lee EB, Kremmer E, Flatley A, Xu Y, et al. Phosphorylation of S409/410 of TDP-43 is a consistent feature in all sporadic and familial forms of TDP-43 proteinopathies. Acta Neuropathol 2009; 117: 137–49.

Ossenkoppele R, Pijnenburg YA, Perry DC, Cohn-Sheehy BI, Scheltens NM, Vogel JW, et al. The behavioural/dysexecutive variant of Alzheimer's disease: clinical, neuroimaging and pathological features. Brain 2015; 138 (Pt 9): 2732–49.

Placek K, Massimo L, Olm C, Ternes K, Firn K, Van Deerlin V, et al. Cognitive reserve in frontotemporal degeneration: neuroanatomic and neuropsychological evidence. Neurology 2016; 87: 1813–19.

Powers JP, Massimo L, McMillan CT, Yushkevich PA, Zhang H, Gee JC, et al. White matter disease contributes to apathy and disinhibition in behavioral variant frontotemporal dementia. Cogn Behav Neurol 2014; 27: 206–14.

Ranasinghe KG, Rankin KP, Pressman PS, Perry DC, Lobach IV, Seeley WW, et al. Distinct subtypes of behavioral variant frontotemporal dementia based on patterns of network degeneration. JAMA Neurol 2016; 73: 1078–88.

Rankin KP, Gorno-Tempini ML, Allison SC, Stanley CM, Glenn S, Weiner MW, et al. Structural anatomy of empathy in neurodegenerative disease. Brain 2006; 129 (Pt 11): 2945–56.

Rascovsky K, Hodges JR, Knopman D, Mendez MF, Kramer JH, Neuhaus J, et al. Sensitivity of revised diagnostic criteria for the behavioural variant of frontotemporal dementia. Brain 2011; 134 (Pt 9): 2456–77.

Rascovsky K, Salmon DP, Hansen LA, Thal LJ, Galasko D. Disparate letter and semantic category fluency deficits in autopsy-confirmed frontotemporal dementia and Alzheimer's disease. Neuropsychology 2007; 21: 20–30.

Rogalski E, Weintraub S, Mesulam MM. Are there susceptibility factors for primary progressive aphasia? Brain Lang 2013; 127: 135–8.

Rohrer JD, Lashley T, Schott JM, Warren JE, Mead S, Isaacs AM, et al. Clinical and neuroanatomical signatures of tissue pathology in frontotemporal lobar degeneration. Brain 2011; 134 (Pt 9): 2565–81.

Rossor MN, Fox NC, Mummery CJ, Schott JM, Warren JD. The diagnosis of young-onset dementia. Lancet Neurol 2010; 9: 793–806.

Seeley WW, Bauer AM, Miller BL, Gorno-Tempini ML, Kramer JH, Weiner M, et al. The natural history of temporal variant frontotemporal dementia. Neurology 2005; 64: 1384–90.

Seeley WW, Crawford R, Rascovsky K, Kramer JH, Weiner M, Miller BL, et al. Frontal paralimbic network atrophy in very mild behavioral variant frontotemporal dementia. Arch Neurol 2008; 65: 249–55.

Stefanits H, Budka H, Kovacs GG. Asymmetry of neurodegenerative disease-related pathologies: a cautionary note. Acta Neuropathol 2012; 123: 449–52.

Suh E, Lee EB, Neal D, Wood EM, Toledo JB, Rennert L, et al. Semi-automated quantification of C9orf72 expansion size reveals inverse correlation between hexanucleotide repeat number and disease duration in frontotemporal degeneration. Acta Neuropathol 2015; 130: 363–72.

Toledo JB, Van Deerlin VM, Lee EB, Suh E, Baek Y, Robinson JL, et al. A platform for discovery: The University of Pennsylvania Integrated Neurodegenerative Disease Biobank. Alzheimers Dement 2014; 10: 477–84.e1.

Tustison NJ, Cook PA, Klein A, Song G, Das SR, Duda JT, et al. Large-scale evaluation of ANTs and FreeSurfer cortical thickness measurements. Neuroimage 2014; 99: 166–79.

Viskontas IV, Possin KL, Miller BL. Symptoms of frontotemporal dementia provide insights into orbitofrontal cortex function and social behavior. Ann N Y Acad Sci 2007; 1121: 528–45.

Whitwell JL, Boeve BF, Weigand SD, Senjem ML, Gunter JL, Baker MC, et al. Brain atrophy over time in genetic and sporadic frontotemporal dementia: a study of 198 serial magnetic resonance images. Eur J Neurol 2015; 22: 745–52.

Whitwell JL, Josephs KA, Rossor MN, Stevens JM, Revesz T, Holton JL, et al. Magnetic resonance imaging signatures of tissue pathology in frontotemporal dementia. Arch Neurol 2005; 62: 1402–8.

Whitwell JL, Przybelski SA, Weigand SD, Ivnik RJ, Vemuri P, Gunter JL, et al. Distinct anatomical subtypes of the behavioural variant of frontotemporal dementia: a cluster analysis study. Brain 2009; 132 (Pt 11): 2932–46.

Woolley JD, Gorno-Tempini ML, Seeley WW, Rankin K, Lee SS, Matthews BR, et al. Binge eating is associated with right orbitofrontal-insular-striatal atrophy in frontotemporal dementia. Neurology 2007; 69: 1424–33.

Xie SX, Baek Y, Grossman M, Arnold SE, Karlawish J, Siderowf A, et al. Building an integrated neurodegenerative disease database at an academic health center. Alzheimers Dement 2011; 7: e84–93.

Yu CE, Bird TD, Bekris LM, Montine TJ, Leverenz JB, Steinbart E, et al. The spectrum of mutations in progranulin: a collaborative study screening 545 cases of neurodegeneration. Arch Neurol 2010; 67: 161–70.